Production Carrying Capacity assessment for offshore mussel culture development in îles de la Madeleine (Québec, Canada)

T. Guyondet, C.W. McKindsey, F. Bourque, A. Drouin, M. Nadeau and A. Weise

Fisheries and Oceans Canada
Gulf Fisheries Centre,
P.O. Box 5030,
Moncton (New Brunswick),
Canada
E1C 9B6

2015

Canadian Technical Report of
Fisheries and Aquatic Sciences 3148

Fisheries and Oceans Canada | Pêches et Océans Canada

Canada

Canadian Technical Report of Fisheries and Aquatic Sciences

Technical reports contain scientific and technical information that contributes to existing knowledge but which is not normally appropriate for primary literature. Technical reports are directed primarily toward a worldwide audience and have an international distribution. No restriction is placed on subject matter and the series reflects the broad interests and policies of Fisheries and Oceans Canada, namely, fisheries and aquatic sciences.

Technical reports may be cited as full publications. The correct citation appears above the abstract of each report. Each report is abstracted in the data base *Aquatic Sciences and Fisheries Abstracts.*

Technical reports are produced regionally but are numbered nationally. Requests for individual reports will be filled by the issuing establishment listed on the front cover and title page.

Numbers 1-456 in this series were issued as Technical Reports of the Fisheries Research Board of Canada. Numbers 457-714 were issued as Department of the Environment, Fisheries and Marine Service, Research and Development Directorate Technical Reports. Numbers 715-924 were issued as Department of Fisheries and Environment, Fisheries and Marine Service Technical Reports. The current series name was changed with report number 925.

Rapport technique canadien des sciences halieutiques et aquatiques

Les rapports techniques contiennent des renseignements scientifiques et techniques qui constituent une contribution aux connaissances actuelles, mais qui ne sont pas normalement appropriés pour la publication dans un journal scientifique. Les rapports techniques sont destinés essentiellement à un public international et ils sont distribués à cet échelon. Il n'y a aucune restriction quant au sujet; de fait, la série reflète la vaste gamme des intérêts et des politiques de Pêches et Océans Canada, c'est-à-dire les sciences halieutiques et aquatiques.

Les rapports techniques peuvent être cités comme des publications à part entière. Le titre exact figure au-dessus du résumé de chaque rapport. Les rapports techniques sont résumés dans la base de données *Résumés des sciences aquatiques et halieutiques.*

Les rapports techniques sont produits à l'échelon régional, mais numérotés à l'échelon national. Les demandes de rapports seront satisfaites par l'établissement auteur dont le nom figure sur la couverture et la page du titre.

Les numéros 1 à 456 de cette série ont été publiés à titre de Rapports techniques de l'Office des recherches sur les pêcheries du Canada. Les numéros 457 à 714 sont parus à titre de Rapports techniques de la Direction générale de la recherche et du développement, Service des pêches et de la mer, ministère de l'Environnement. Les numéros 715 à 924 ont été publiés à titre de Rapports techniques du Service des pêches et de la mer, ministère des Pêches et de l'Environnement. Le nom actuel de la série a été établi lors de la parution du numéro 925.

Canadian Technical Report of
Fisheries and Aquatic Sciences 3148

2015

PRODUCTION CARRYING CAPACITY ASSESSMENT FOR OFFSHORE MUSSEL CULTURE DEVELOPMENT IN ÎLES DE LA MADELEINE (QUÉBEC, CANADA)

by

T. Guyondet[1], C.W. McKindsey[2], F. Bourque[3], A. Drouin[2], M. Nadeau[4] and A. Weise[2]

Fisheries and Oceans Canada
Gulf Fisheries Centre,
P.O. Box 5030,
Moncton (New Brunswick),
Canada
E1C 9B6

[1] Fisheries and Oceans Canada, Gulf Fisheries Centre, P.O. Box 5030, Moncton (New Brunswick), Canada E1C 9B6
[2] Fisheries and Oceans Canada, Maurice Lamontagne Institute, 850 route de la Mer, P.O. Box 1000, Mont-Joli (Québec), Canada G5H 3Z4
[3] Ministère de l'Agriculture, des Pêcheries et de l'Alimentation du Québec. Direction générale des pêches et de l'aquaculture commerciales, 101-125 chemin du Parc, Cap-aux-Meules (Québec), Canada G4T 1B3
[4] Merinov - Centre des Îles-de-la-Madeleine, 107-125 chemin du Parc, Cap-aux-Meules (Québec), Canada G4T 1B3

© Her Majesty the Queen in Right of Canada, 2015.
Cat. No. Fs 97-6/3148E-PDF ISBN 978-0-660-03878-0 ISSN 1488-5379

Correct citation for this publication:

Guyondet, T., McKindsey, C.W., Bourque, F., Drouin, A., Nadeau, M., and A. Weise. 2015. Production carrying capacity assessment for offshore mussel culture development in îles de la Madeleine (Québec, Canada) Can. Tech. Rep. Fish. Aquat. Sci. 3148: vii + 35 pp.

TABLE OF CONTENTS

Page

LIST OF FIGURES iv
ABSTRACT vi
RÉSUMÉ vii
INTRODUCTION 1
MATERIAL AND METHODS 2
STUDY AREA 2
MODELLING 3
Hydrodynamics 3
Farm-scale mussel production model 4
Bay-scale seston depletion model 5
RESULTS AND DISCUSSION 7
WATER COLUMN VERTICAL STRUCTURE 7
HYDRODYNAMICS 7
Model validation 7
Water renewal time 8
MUSSEL GROWTH VALIDATION 8
EFFECTS OF FARM DESIGN ON PRODUCTION AND FOOD RESOURCES 8
DEPLETION DIAGNOSTIC FOR FUTURE MUSSEL CULTURE DEVELOPMENT 11
CONCLUSIONS 12
ACKNOWLEDGEMENTS 13
REFERENCES 13

LIST OF FIGURES

Page

Figure 1. Map of the study area showing the bathymetry within the Baie de Plaisance (BdP) hydrodynamic model domain and the location of the aquaculture development zone (ADZ; red polygon). 17

Figure 2. Sketch of typical farm layout currently used by the commercial mussel farm in BdP. 18

Figure 3. Location of the 2001 tide gauges (L1, 9, 10, 11, 12) from Guyondet and Koutitonsky (2008) and 2013 current meters, CTD and water sampling stations (ADCP1 and 2). The contours of the ADZ (dashed line) and of the farm currently in operation (bold line) are also reported. 19

Figure 4. Vertical profiles of water temperature (top panel) and salinity (bottom panel) at station ADCP2 during the whole 2013 sampling period. 20

Figure 5. Comparison of tidal current time series at the top and bottom of the water column at station ADCP2 during the month of June 2013. 21

Figure 6. Sketch of farm-scale model configuration with x axis oriented along the longlines and box dimensions (length BL = 1/10 of longline length (L), width or line spacing w and mussel sock length BH) for which current velocity (v) and seston concentration (P) are calculated. 22

Figure 7. Time series of environmental conditions (water temperature, phytoplankton concentration (Chl a) and current velocity) used to force the farm-scale model and obtained from the analysis of CTD, ADCP current meter, and water sample data collected at station ADCP2 during summer-fall 2013. 23

Figure 8. Shell length – Individual dry weight relation for all individual mussels collected during the course of the 2013 field study for growth measurements. The relationship Volume (V) – Shell length (SL) used in the Dynamic Energy Budget (DEB) is also reported for the calibrated value of the shape parameter (δ). 24

Figure 9. Mean vertical structure of the water column during the study period at station ADCP2 in terms of water temperature (top left panel) and phytoplankton concentration (measured as fluorescence, top right panel). These observations are reported for 3-m depth ranges with 0.5 m increments and expressed as relative variation compared to the 9-12 m layer. The bottom panel gives the vertical structure in mean (Root Mean Square, RMS) current velocity at 1 m intervals..... 25

Figure 10. Hydrodynamic model validation. Comparison of observed and predicted tidal water level fluctuation time series at station L12 during the month of June 2001. 26

Figure 11. Spatial distribution of water renewal time over BdP from the hydrodynamic model results and the tracer advection-dispersion method. 27

Figure 12. DEB model validation. Comparison of observed and predicted mussel growth both in terms of shell length (top panel) and dry meat weight (bottom panel). Mean observed values are reported along with ± 1 standard deviation. 28

Figure 13. Distribution of food depletion along a typical longline corridor as reproduced by the farm-scale model in response to the combine effects of food replenishment by water circulation and food consumption by mussel filtration. Food depletion is calculated as the relative difference between food concentration inside the farm and the outside forcing concentration. 29

Figure 14. Farm-scale model results. Effects of stocking density and longline spacing (w) on total farm yield (top panel) and individual mussel growth (bottom panel) reported as the shell length at the end of the simulation period (error bars represent spatial variability within the farm and for clarity are only included for the minimum, maximum and current line spacing scenarios). Farm yield and final shell length obtained at w = 50 m are indicated (dotted lines) for both current and maximum production scenarios. The planned configuration (L = 120 m and w = 50 m) is also presented (dashed red line)..... 30

Figure 15. Farm-scale model results. Effects of longline length (L) and stocking density on total farm yield (top panel; see text for broken line meaning) showing the optimum reached for L = 120 m (longline length planned with technological development). Effects of longline length and spacing on total farm yield (bottom panel) also showing optimum for L = 120 m and spacing w < 60m. 31

Figure 16. Depletion model results. Effects of 4 isolated typical farms on the spatial distribution of food depletion in three sock spacing scenarios (44, 55 and 65 cm). Food depletion is expressed as the seston depletion index SDI. SDI > 0 denotes an actual depletion while SDI <0 follows an accumulation of seston compared to the boundary constant value. Black polygons delineate the farms. 32

Figure 17. Depletion model results. Spatial distribution of SDI over BdP for the case where the typical farm design is extended over the whole ADZ and for the three sock spacing scenarios. Red contours delineate the maximum extent of depletion (SDI > 0) predicted over the course of the simulation period. 33

Figure 18. Depletion model results. Spatial distribution of SDI over BdP for the case where the typical farm design is extended over the whole ADZ with twice the baseline stocking density and for the three sock spacing scenarios. Red contours delineate the maximum extent of depletion (SDI > 0) predicted over the course of the simulation period..... 34

Figure 19. Depletion model results. Spatial distribution of SDI over BdP for the case where the typical farm design is extended over the whole ADZ with three times the baseline stocking density and for the three sock spacing scenarios. Red contours delineate the maximum extent of depletion (SDI > 0) predicted over the course of the simulation period..... 35

ABSTRACT

Guyondet, T., McKindsey, C.W., Bourque, F., Drouin, A., Nadeau, M., and A. Weise. 2015. Production carrying capacity assessment for offshore mussel culture development in îles de la Madeleine (Québec, Canada) Can. Tech. Rep. Fish. Aquat. Sci. 3148: vii + 35 pp.

Moving bivalve aquaculture activities offshore alleviates to some degree all of the constraints encountered in near-shore areas. Consequently, further development of this industry in îles de la Madeleine is planned offshore in Baie de Plaisance. The characterization of production potential in that area constitutes a critical step in the development process.

The present project aimed at estimating the production carrying capacity of this offshore site for mussel culture. Numerical modelling tools were built on *in situ* data to reproduce cultured mussel growth and sestonic food availability as well as to simulate scenarios of future development.

Combining both the farm- and bay-scale evaluations, it was concluded that a scale-up of current stocking levels to the whole designated site with an additional 150 % would still be within the limits of the production carrying capacity of Baie de Plaisance.

RÉSUMÉ

Guyondet, T., McKindsey, C.W., Bourque, F., Drouin, A., Nadeau, M., and A. Weise. 2015. Production carrying capacity assessment for offshore mussel culture development in îles de la Madeleine (Québec, Canada) Can. Tech. Rep. Fish. Aquat. Sci. 3148: vii + 35 pp.

Le déplacement des activités conchylicoles vers le large permet en théorie de réduire la plupart des contraintes rencontrées dans les régions proches de la côte. Dans ces conditions, aux îles de la Madeleine, le développement de cette industrie se planifie au large dans la Baie de Plaisance. L'évaluation du potentiel de production dans cette région constitue donc une phase critique dans le processus de développement.

Le projet présenté dans ce rapport visait à estimer la capacité de production pour la mytiliculture de ce nouveau site au large. La croissance des moules en culture ainsi que la disponibilité de leur nourriture a été reproduite à l'aide d'outils de modélisation numérique basés sur des observations de terrain. Ces modèles ont également permis de simuler de futurs scénarios de développement de l'industrie.

L'approche combinant des évaluations à l'échelle de la ferme et de la baie a permis de conclure que l'activité mytilicole, avec les densités d'élevage utilisées aujourd'hui, pouvait être étendue à la totalité du site identifié et même intensifiée de 150 % sans que la capacité de production de la Baie de Plaisance ne soit dépassée.

INTRODUCTION

The worldwide development of bivalve aquaculture faces various constraints in near-shore areas, either due to space limitation (physical carrying capacity), production limitation due to food availability (production carrying capacity), ecosystem-scale impacts amplified by slow water flushing (ecological carrying capacity) and development limitation due to other uses (social carrying capacity) of the receiving system (Inglis et al. 2000, McKindsey et al. 2006). Moving bivalve aquaculture activities offshore, a more and more viable option as proper technological developments become available (Stevens et al. 2008), alleviates to some degree all of the above mentioned constraints. For example, moving culture sites to offshore locations greatly increases the area in which bivalves may be grown, both in terms of surface area as well as volume (i.e. a deeper water column may be used to grow the bivalves), thus limiting physical carrying capacity issues. Production capacity may also be less of an issue with respect to *in situ* bivalve food production as renewal of resources through water exchange may occur more rapidly. To date, most work on determining the production carrying capacity of sites for bivalve culture has concentrated on coastal embayment systems in which organic seston is a limiting resource due to restricted water transport and exchange (Guyondet et al. 2013). Less work has been done in more open, offshore locations, where *in situ* primary productivity may be less important than hydrodynamics for seston renewal (but see Ferreira et al 2009). With respect to ecological carrying capacity, greater reliance on direct resource renewal (i.e. advection of sestonic food resources) than *in situ* production may limit impacts on the surrounding pelagic ecosystem and cascading effects from this. At the same time, greater dispersive capacity and resuspension in offshore areas due to greater hydrodynamic forces may limit benthic effects, as has been shown in a variety of studies (Giles et al. 2009; Weise et al. 2009). Moving bivalve culture offshore also improves the social license of this industry insomuch that there is less competition for high valued coastal areas (e.g. with boaters, visual impact; Department of Marine and Natural Resources 2001; Goulletquer and Le Moine 2003), although this may also increase competition for space with fisheries and other offshore activities (Longdill et al. 2008; Stead et al. 2002).

In îles de la Madeleine, eastern Canada, bivalve aquaculture, mainly blue mussels (*Mytilus edulis*), started in the 1980's in the two main lagoons of the archipelago. The limited extent of areas deep enough to accommodate traditional longline mussel culture inside the lagoons has forced producers and managers to consider offshore sites to further the development of this industry. A siting exercise was undertaken to identify potential growing sites based on spatial planning activities using GIS tools (Werstink 2007), discussions with local stakeholders, and growth trials (Bourque and Myrand 2014). This approach adequately covered the physical and social aspects of the carrying capacity for mussel aquaculture in the area. However, the exercise only provided preliminary

information on potential production carrying capacity, in terms of feasibility, mussel growth potential, and potential intensity and extent of production.
The present contribution reports the results of various numerical models built on *in situ* data to estimate the production carrying capacity for mussel aquaculture of an offshore site in îles de la Madeleine while accounting for both farm- and bay-scale interactions between the cultured mussels and natural food resources. A basic model is first presented and then this is used to explore the effects of farm design on production and food resources and to be used as a diagnostic tool for future mussel culture development.

MATERIAL AND METHODS

STUDY AREA

The area of interest is îles de la Madeleine, Québec, eastern Canada, in the southern Gulf of Saint-Lawrence (GSL, Fig. 1). The present study covers the whole Baie de Plaisance (BdP) and extends further to the south-southeast in the GSL. The presence of an amphidromic point for the main semi-diurnal tide near the archipelago (Godin 1979) leads to a weak tidal forcing in BdP with amplitudes ranging between 0.1 and 0.5 m from neap to spring tides (Koutitonsky et al. 2002). While a thick consolidated ice sheet covers the lagoons in winter, drifting ice is more common offshore. Moreover, predominant westerly winds (Drapeau 1988) push the ice further offshore and the study area stays free of ice for extended periods of time (Bourque and Myrand 2014). The siting exercise performed by Werstink (2007) identified an area of about 13 km^2 (2.7 × 5 km) just North of BdP (marked by the polygon in Fig. 1) that is presently considered by the Québec government to become an aquaculture development zone (ADZ) to facilitate and expedite the allocation of leases for bivalve culture. All analyses done in the present study are based on this configuration. Depths in the ADZ average 18 m. Following several years of an experimental culture phase during which several longline and farm designs were tested, a commercial farm is now operating in that area. The company chose the most manageable layout where 100-m longlines are set 50 m apart along a northeast-southwest direction and rows of longlines are separated by 90-m buffer zones imposed by the length of mooring lines at each end (2 x 45 m). This design leads to a final density of one longline per hectare of farm (Fig. 2a). Each line is sunk at about 9 m below the surface and supports 180 vertical mussel socks (55 cm apart) of 3 m length. The target of 700 mussels per meter of sock brings the mussel density in the farmed area to about 37.8 ind m^{-2} and also translates into 1273 ind m^{-2} of vertical wall created by the mussel socks. About 2/3 of the mussel seed is collected in the Bassin du Havre-Aubert (BHA), a small lagoon located at the southern end of the archipelago (Fig. 1), and the remainder on-site in the BdP farm. In the present study, no distinction was made between the two stock origins. Mussels are seeded in the growing site each year in the fall (October-November) and usually reach a harvestable size of 55 mm shell length late the next fall (~18 mo old mussels). As a consequence of the growing period extending over more than 1

yr, a maximum of 50% of the farm area can be attributed to a given cohort. Mussels in BdP are known to spawn in early June – about 2-3 weeks later than those in the lagoons (Gauthier-Clerc et al. 2007; Bourque and Myrand 2014).

MODELLING

The production carrying capacity of an area for bivalve aquaculture may be determined by considering effects occurring at three time scales (Dame and Prins 1997). The availability of food resources may be described by the combination of the time taken for organic seston to be renewed by local primary production (i.e. seston turnover time) and the time taken by hydrodynamic forces to renew the water mass in the area of interest (i.e. water renewal time). The last time scale relates to the rate of food consumption by the farmed bivalves (i.e. clearance time). The relative importance of these three processes in setting the food production-consumption balance may vary depending on the spatial scale considered (Guyondet et al. 2010). The methodology applied in the present study integrates the three processes at two relevant spatial scales. The farm-scale allows for testing the effects of different farm designs on net productivity. A factorial design was used to set up scenarios of the farm-scale model based on the three parameters: longline length (L), longline spacing (w) and mussel density along the longlines (d). The bay-scale (henceforth referred to as BdP) accounts for cumulative effects of multiple farms and provides insight into potential farm interactions. This aspect was addressed using a seston depletion approach (Guyondet et al. 2013) based on the results of a spatially explicit hydrodynamic model and a combination of mussel culture extent and intensity scenarios. The different modelling frameworks are detailed in the next sections.

Hydrodynamics

The characterization of both farm- and bay-scale hydrodynamics is necessary to determine site-specific water renewal time scales. At the local-scale, this was achieved by deploying two ADCP current meters (Workhorse Sentinel, Teledyne RD Instruments, Poway, CA, USA) in the vicinity of the commercial farm (Fig. 3) from June to October 2013 to record current speed and direction every 30 min at 1 m intervals over the whole water column.

ADCP data were also combined with vertical profiles from a CTD (SBE-19plus, Sea-Bird Electronics, Bellevue, WA, USA) and a fluorometer (to estimate phytoplankton biomass) to characterize the vertical structure of local environmental conditions in the mussel production area.

A numerical model was developed to address bay-scale variation in hydrodynamics within BdP. This included a RMA-10 finite element model (King 1982) to reproduce tidal hydrodynamics in BdP. Tidal water level fluctuations at stations L1, L9, L10, L11 and L12 (Fig. 3) were extracted by harmonic analysis (Foreman 1977) from tide gauge data collected in summer 2001 (see Guyondet and Koutitonsky 2008 for more details) and were used to force the model along its open boundaries (out in the GSL and at the Havre-aux-Maisons Lagoon

(HML) and Grande-Entrée Lagoon (GEL) inlets) and validate model results. CTD vertical profiles collected in the farm area during summer-fall 2013 show no sign of long-term vertical stratification in temperature or salinity except for a few weeks in late August – early September (Fig. 4). Moreover, the decomposition along their principal axis shows that tidal currents in the upper and lower parts of the water column have a similar orientation (234° and 248° anti-clockwise from East, respectively) and are in phase (Fig. 5). Consequently, there is no major vertical variation in tidal circulation. Hence, a two-dimensional depth-averaged representation of the system was used to reproduce the main tidal hydrodynamic features of BdP. The model was then used to compute the water renewal time distribution in BdP, i.e. the time taken for the water at any location in the bay to be renewed by water from the outside (GSL, HML or GEL), following the tracer advection-dispersion method described by Koutitonsky et al. (2004).

Farm-scale mussel production model

Carrying capacity and interactions within the farm were estimated using the model developed by Rosland et al. (2011). The model includes a representation of corridors located between two adjacent longlines which is described using 10 boxes of uniform dimensions defined by longline spacing (w), the length of mussel socks (B_H) and 1/10 longline length (B_L, Fig. 6). Assuming the system is in steady-state and boundary conditions are known, the model estimates decreases of currents due to the drag from mussel socks and particulate food transport and consumption by mussels along the corridor. Filtration by mussels is derived from an ecophysiological sub-model based on Dynamic Energy Budget (DEB) theory (Kooijman 2000). The DEB for *Mytilus edulis* (described in detail by Rosland et al. 2009) predicts the growth of a generic individual both in terms of shell length and meat weight for prescribed environmental conditions, i.e. food concentration (calculated by the transport model along the corridor) and water temperature (input as a forcing). The farm yield is derived by scaling up the model results, i.e. adding longline corridors to reach the farm width desired. The effects of various farm designs can then be tested with respect to both individual mussel growth and farm yield.

Current boundary conditions for the farm-scale model were extracted from the ADCP data collected closest to the commercial farm (ADCP2, Fig. 3). Currents were averaged over the depth cells corresponding to the position of the mussel socks in the water column (9-12 m below the surface). It may be noted that the orientation of the current principal axis reported (234-248° from East) aligns well with the orientation of the commercial longlines (240° from East). The currents were then projected along this direction to serve as input to the farm-scale model (Fig. 7). Chlorophyll *a* (chl *a*) concentrations were used as a proxy for mussel food. Water samples were collected outside the farm close to station ADCP2 (Fig. 3) once every two weeks (June-August 2013) or once a month (September, October, and November 2013) at the depth of mussel socks. Subsamples (500 mL) were filtered in triplicates (Whatman GF/C filters) and analysed for chl *a* following Strickland and Parsons (1972). Water temperature forcing was obtained

from a CTD probe (SBE-19plus) deployed at station ADCP2 at the depth of mussel socks for the whole period (June - October). The model uses a daily time step to ensure the steady-state condition is met. The boundary and forcing conditions reproduced in Fig. 7 were then either averaged daily (currents and temperature) or linearly interpolated (chl *a*) to be implemented in the model calculations. Although there is no guarantee chl *a* concentration used for boundary conditions was not affected by the presence of the farm, the location of the sampling station outside the farm limited this possibility. In any case, this would result in a worst-case scenario in terms of food availability and hence, a precautionary approach to carrying capacity assessment.

DEB model results were validated using *in situ* mussel growth measurements. To validate growth rates, all mussels from a 10-cm long mussel sock section were collected from each of 5 different socks randomly chosen on an experimental line deployed just north of the commercial farm once every two weeks from June to August and then once a month from September to November. At least 30 mussels from each sock sample were randomly selected for measurement of shell length (to the nearest 0.01 mm) and meat dry weight (after desiccation at 70 °C for 24 h). Two of the DEB model parameters had to be adapted to the studied population (shape coefficient, δ) and site conditions (food half saturation coefficient, K_F^M). The shape coefficient relates the shell length (SL, cm) to the structural volume (V, cm^3) of the mussels as:

$$\delta = \frac{V^{1/3}}{SL} \qquad (1)$$

This parameter was estimated from measurements of shell length and dry meat weight of 450 mussels collected from socks on 14 August 2013. At that time, mussels are thought to have completed spawning and were the thinnest compared to other sampling dates (Fig. 8), total dry weight was then the closest to structural weight. The dry meat weight (DW) observations were converted to volumes using a dry to wet weight ratio of 0.2 and a wet weight to volume ratio of 1 g cm^{-3} (Rosland et al. 2009). Mussel meat contains not only structural tissues but also energy reserves and gonads. Hence, the method described in Rosland et al. (2009) was used to adjust δ such that only 5% of all observations fall below the volume-length curve described by Eq. 1. This procedure gave $\delta = 0.268$.

The mussel model parameter K_F^M was calibrated within the farm-scale model framework by comparing observed and predicted data of individual shell length and dry meat weight for the baseline scenario described below.

The farm-scale model was set-up to reproduce the baseline scenario that corresponds to the farm design described in section "Study area" and in Fig. 2. The response of total farm yield and individual mussel growth was then investigated for various farm designs by altering longline length and spacing and various stocking densities by changing the sock spacing along longlines.

Bay-scale seston depletion model

The methodology described by Guyondet et al. (2013) was used to reproduce the dynamics of organic seston in BdP under the influence of the three driving

processes mentioned earlier, i.e. primary production, water circulation, and mussel filtration. Briefly, a suspended variable module representing organic seston was coupled to the hydrodynamic model via the convection-diffusion equation:

$$\frac{\partial P}{\partial t} + u\frac{\partial P}{\partial x} + v\frac{\partial P}{\partial y} = \frac{\partial}{\partial x}\left(D_x\frac{\partial P}{\partial x}\right) + \frac{\partial}{\partial y}\left(D_y\frac{\partial P}{\partial y}\right) + \alpha - \beta P \qquad (2)$$

where P is the organic seston concentration in mgC m^{-3}, u and v are the current speeds in direction x and y, respectively, calculated by the hydrodynamic model, D_x and D_y are the dispersion coefficients proportional to u and v, respectively, α is the phytoplankton primary production rate in mgC m^{-3} d^{-1} and β is the bivalve population clearance rate in times per day

The same sampling protocol as for chl *a* was used for organic seston. Triplicate subsamples (1 L) were filtered (pre-weighed and burnt Whatman GF/F filters) and the filters dried (70 °C for 24 h) to determine total suspended matter concentrations (TPM) and burnt (500 °C for 4 h) to determine particulate organic matter concentrations (POM). A 33% carbon content was used to convert POM to particulate organic carbon concentrations (POC) according to observations made in the southern GSL in summer 2012 and 2013 (Guyondet, unpublished data). The uniform initial concentration and constant boundary conditions used for all depletion model simulations were set to P_0 = 429 mg C m^{-3}, the mean value observed during the study period in BdP.

The primary production rate α was estimated from *in situ* measurements made during summer-fall 2004 in GEL using the ^{14}C method (Trottet et al. 2007). Its value was kept uniform over the model domain and constant during the simulation period and corresponded to a planktonic primary production rate of 100 g C m^{-2} yr^{-1}, a typical rate in temperate coastal systems (Heip et al. 1995).

The bivalve population clearance rate was calculated as the product of individual bivalve clearance rates (m^3 ind^{-1} d^{-1}) and density of bivalves in the farm area (ind m^{-2}) and divided by depth. The individual clearance rate was fixed to 3.9 L h^{-1}, the averaged value observed for mussels of 3 – 6 cm shell length in Prince Edward Island (L. Comeau, pers. comm.), about 125 km from the study site. Various stocking density scenarios were tested, in particular the baseline scenario described above.

To investigate the cumulative effects of multiple farms and the interactions between farms, two spatial configurations were evaluated. The cumulative tests assumed mussel aquaculture was fully developed with a uniform mussel density (as described for the current situation in section "Study area") throughout the ADZ, while the farm interaction tests considered only 4 farms of typical design (Fig. 2) distributed in the ADZ, one at each corner.

All simulations covered a 48-day period. Results were compiled as an organic seston depletion index (SDI, Guyondet et al. 2013). SDI is expressed as a percent change in seston concentration relative to the boundary concentration (P_0). To allow the seston concentration to reach an equilibrium state in the farmed areas, results were recorded starting 5 days after the start of the simulation. The concentration was then averaged over the remainder of the

period at each node *i* of the model domain and this averaged concentration P_{avg} compared to the boundary value to estimate SDI as follows:

$$SDI(i) = 100 \times \frac{P_0 - P_{avg}(i)}{P_0} \qquad (3)$$

Positive SDI values denote a decrease in organic seston availability due to bivalve filtration, whereas negative SDI values reveal seston accumulation due to local primary production in less flushed areas.

RESULTS AND DISCUSSION

WATER COLUMN VERTICAL STRUCTURE

As stated earlier, the water column presented no stratification during most of the mussel growing period in BdP (Fig. 4). ADCP data and CTD (equipped with a fluorometer) profiles were analyzed to further explore the vertical structure of key components for mussel production, i.e. water temperature, food concentration and current speed (Fig. 9). Temperature and fluorescence (a measure of phytoplankton biomass used as a proxy for mussel food) data were averaged over the study period and a moving mean with 0.5 m increments was applied to these averaged profiles to calculate mean conditions over 3-m depth ranges (length of mussel socks). The 9-12 m range, corresponding to the layer where mussel socks are currently deployed, experienced a mean temperature of 13.3 °C over the study period. This layer was used as reference to compute the relative difference with all other 3-m layers. Despite the dominance of well-mixed conditions, periods of stratification lead to the presence of a vertical structure in mean conditions. Figure 9 (top panels) show opposite gradients of temperature and food concentration over the water column. The mean conditions in BdP are characterized by warmer/poorer (i.e. poorer with respect to fluorescence) water close to the surface and cooler/richer water near the bottom. In terms of mussel growth, richer bottom layers could provide better conditions. This improvement would however be compensated, at least partially, by the colder temperatures. Moreover, root mean square (RMS) current speed does not vary much vertically, except for the surface layer, which is subject to direct wind forcing (Fig. 9, bottom panel). Mussel socks cannot be deployed in the surface layer to enable navigation and prevent damage from drifting ice during the winter. According to these observations, unless mussel density was such that individual growth was strongly food limited, no major gain in mussel production is expected from any change in the vertical position of the stock.

HYDRODYNAMICS

Model validation

Comparison of observations and model predictions of water levels at station L12 shows the good performance of the model (Fig. 10, overall RMS error = 3.6 cm).

Given the location of L12 in the innermost part of the domain, this good agreement indicates that the model reproduces the tidal propagation accurately over the whole domain.

Water renewal time

The distribution of water renewal time over BdP is shown in Fig. 11. As can be expected, the further away from a boundary, the longer it takes for the water to be renewed from outside of the domain with a maximum duration longer than 48 days in the innermost area close to station L12. In the ADZ, renewal times range from 25 to 40 days with a positive East - West gradient. This result is influenced by the model set-up where the GSL boundary is closer to the eastern side of the ADZ. Nonetheless, this gradient indicates that water exchange is reduced in the E-W direction which is in agreement with the earlier observation that the principal current axis in this area is quasi perpendicular to this E-W direction.

MUSSEL GROWTH VALIDATION

The best agreement between DEB predicted and observed growth was reached for K_F^M = 60 mg C m^{-3} or 1.2 µg Chl *a* L^{-1}. Shell growth is well reproduced by the model (Fig. 12, top panel) while meat weight increase seems to be slightly overestimated right after spawning and underestimated in late summer and early fall (Fig. 12, bottom panel). A 38.4% spawning threshold for the gonado-somatic index (ratio of gonad dry weight to total dry weight) best reproduced the timing of the observed spawning event between the two first dates of the sampling period (7 and 18 June). This threshold value lies well within the 30-40 % range of reported gonado-somatic ratios for *Mytilus edulis* just before spawning (van der Veer et al. 2006). Overall, model results fall within or very close to the limits of observed variability in meat weight and most importantly, are within these limits at the end of the growing season when the farm yield was evaluated in the following farm-scale model applications.

EFFECTS OF FARM DESIGN ON PRODUCTION AND FOOD RESOURCES

An example of food depletion (same calculation as SDI, Eq. 3) along the corridor reproduced by the farm-scale model is given in Fig. 13 for the baseline design (longline length, L = 100 m; longline spacing, w = 50 m; sock length = 3 m; sock spacing of 55 cm and sock density = 700 ind m^{-1} leading to a mussel density d = 1273 ind m^{-2} on the vertical walls of the corridor) and the observed boundary conditions reported in Fig. 7. This illustrates the net effect of water exchange and mussel filtration on the availability of food resources. The maximum depletion occurs closer to the southwestern (SW) end of the lines as a result of the residual current flowing from the northeast (NE) to the southwest (principal axis: 234-248° from East). A local maximum food depletion just above 7% can be considered low in comparison to values predicted for the mussel farm in Grande-Entrée Lagoon (15% at bay-scale which would translate in an even stronger depletion

locally; Guyondet et al. 2010) or observations from other longline farms and mussel rafts (20 – 50%; Strohmeier et al. 2005, Petersen et al. 2008).

Farm yield over the simulation period (June-October) was calculated as the difference between the initial and final stock of mussels. These total stocks were obtained by extrapolating the stock in a corridor, first to a row of longlines (the number of longlines in a row being set by farm width and line spacing) and then to the number of rows in a farm (set by ½ farm length (at most 50% of the lines in a farm are used for the harvestable cohort), line length and length of mooring lines; Fig. 2). The first step assumes that all lines in a row are subject to the same boundary conditions. There is no evidence that this assumption does not hold in BdP where no major difference in currents and CTD data were observed between the two ADCP stations. Thus, conditions can be considered as homogenous over a 1 km^2 scale. The second step assumes that all rows of lines in a farm are also subject to the same boundary conditions. This assumption is more difficult to ascertain as the cultured mussel effects are mostly propagated in the lines direction, hence two consecutive rows might influence each other. This assumption is thus equivalent to assuming that the void between rows is wide enough and mixing strong enough that background conditions are restored from the end of one line to the beginning of the line in the next row. Petersen et al. (2008) studied the food depletion caused by a mussel raft in an area with similar current velocity as BdP and noticed that the strong depletion (up to 40%) observed within the raft rapidly decreased at a reference station located 30 m downstream. They concluded that the 100 m spacing between the rafts was optimal for the use of available space and replenishment of food between the consecutive rafts. Both the current reduction and food depletion are expected to be much lower in a longline culture farm as water can flow more freely and local mussel density is lower than in a raft. Results of the present model actually show that depletion levels similar to raft observations (Petersen et al. 2008) are only reach for the maximum density scenario defined below (d = 4000 ind m-2) and narrowest line spacing (w = 10 m). Hence, for all scenarios tested up to this extreme and given the preponderance of hydrodynamics at farm-scale, 80-100 m spacing between consecutive rows of longlines is likely sufficient to allow the replenishment of food to background levels and limit interactions between consecutive rows.

The effects of stocking density (sock spacing and density on the socks) and line spacing on farm yield and individual mussel growth are shown in Fig. 14. Except for very narrow line spacing (w < 30 m), the maximum yield is close to 150 t of meat wet weight irrespective of line spacing. This value can be referred to as the maximum production capacity of a 1 km by 1 km farm in BdP. The stocking density at which this maximum is reached increases with increasing line spacing because wider line spacing leads to an overall reduction in the number of lines in a farm. Using the line spacing currently in place (w = 50 m), the maximum yield that can be reached (150.6 t) is more than 3.5 times greater than the predicted current production (42.1 t) for a stocking density more than 7 times that presently used (9450 versus 1273 ind m^{-2}). However, at such a density the individual growth of mussels is depressed to a final shell length of 50.4 mm compared to

53.4 mm for the present stock. This 3 mm difference corresponds to the standard deviation of observed shell lengths in October 2014. The model thus predicts significantly smaller mussels under these high density conditions, suggesting that an extended growing period would be needed for mussels to reach the harvestable size. A more reasonable increase in density to about 4000 ind m^{-2} would keep the final shell length within half a standard deviation compared to present conditions and the farm yield would nonetheless be increased by a factor of 2.5. It is important to note that this theoretical maximum scenario could not be achieved with present culture technique. Mussel density on a sock cannot be increased due to self-thinning (increased fall-off due to space and food limitation; Fréchette and Lefaivre 1990) and sock spacing would have to be reduced 3-fold, which is not physically possible.

To further investigate the effects of farm design, various longline lengths were evaluated in conjunction with different stocking densities (Fig. 15, top panel) or line spacings (Fig. 15, bottom panel). Lines of constant stocking density (Fig. 15, top) were broken at L = 125 m and L = 175 m to show that, at a fixed farm length and row spacing, an increased line length does not necessarily translate into increased stock due to limited space. In these particular instances, the number of rows must be reduced to accommodate the longer lines and the cumulative line length in the farm is reduced compared to the previous length scenario. For any given stocking density, the farm yield reaches an optimum at an intermediate longline length, which represents the best trade-off between maximized farm stock and minimized food depletion (or maximized individual growth).

Row spacing is determined by the length of mooring lines. A new anchorage system is presently under development (F. Bourque, pers. comm.) that would allow using 120-m longlines with the same farm layout by reducing row spacing to 80 m. This particular scenario was reproduced. According to model results, it proved to be the optimal design for BdP conditions at all stocking densities except the two lowest (Fig. 15, top panel). This design also maximizes farm yield for most of the line spacing scenarios tested (Fig. 15, bottom panel). It is only surpassed by the longest line design (L = 400 m) when combined with the wider line spacings (w > 60 m). Under current stocking density conditions (w = 50 m and d = 1273 ind m^{-2}), the model predicts a 17 % increase in production (from 42.1 to 49.4 t) if longline length is extended from 100 to 120 m. At the maximum density evaluated in the present study (d = 3937 ind m^{-2}), extending the longlines from 100 to 120-m length further reduces individual mussel growth (Fig. 14, bottom panel). However, the final shell length for this "maximum" scenario (L = 120 m, d = 3937 ind m^{-2}) remains within one standard deviation of the final length in the baseline scenario (L = 100 m, d = 1273 ind m^{-2}). At this higher stocking density, the model predicts a further 12 % increase in farm production (from 103.9 to 116.5 t) when longlines are extended from 100 to 120 m.

DEPLETION DIAGNOSTIC FOR FUTURE MUSSEL CULTURE DEVELOPMENT

While the farm-scale model provides valuable information for tuning the farm design to available food resources, the management of aquaculture development in the designated ADZ would benefit from a larger scale approach that includes between-farm interactions and cumulative effects. To this end, the depletion diagnostic method was applied to produce maps of the spatial distribution of mean food depletion over BdP. Given the simplifications of seston dynamics in Eq. 2, SDI is not a direct measure of food reduction that could be observed *in situ*. SDI must rather be seen as a relative index showing areas of potential imbalance between sestonic food replenishment by primary production and transport, and consumption by mussels.

First, potential farm interactions were tested by distributing only 4 farms in the whole ADZ. In addition to the baseline scenario (55 cm sock spacing), two other stocking density were tested that corresponded to sock spacing of 44 and 65 cm respectively. Irrespective of the stocking scenario, isolated farms have virtually no effect on food availability (Fig. 16).

The cumulative effect of having a fully developed mussel culture activity was tested by filling the ADZ with three different stock levels corresponding to the baseline scenario (37.8 ind m^{-2} of surface area), twice the baseline, and three times the baseline. This last scenario corresponds to the same stocking level as the maximum theoretical production capacity identified at the farm-scale (d = 3937 ind m^{-2} on corridor walls). The higher stocking scenarios could only be achieved by increasing mussel sock length. In combination with these stocking scenarios, the three sock spacing configurations (44, 55 and 65 cm) tested for farm interactions were also evaluated. The baseline scenario does not lead to depletion of mean food concentrations (SDI remains negative) for any of the sock spacing tested (Fig. 17). Moreover, the maximum extent of transient depletion barely exceeds the ADZ area (red contour in Fig. 17). Low intensity depletion (< 10%) only starts to show when the stocking density is doubled and sock spacing is reduced to 44 cm (Fig. 18). The last scenario considers a 3-fold increase in stocking density. Again this represents a theoretical maximum that could not be reached with present culture techniques, as 3-times longer mussel socks would be too close to touching the bottom. In this extreme scenario, mean depletion reaches 11 to 31% depending on the sock spacing (Fig. 19). The maximum extent of depletion marked by the red contour also covers an area much wider than the ADZ and stretches more in the NE-SW direction as could be expected from the preponderant current direction in this region. However, even for this extreme scenario, food depletion outside the ADZ occurs only for short periods of time and does not persist on longer (months) time scales (i.e. SDI positive values restricted to the ADZ; Fig. 19). Overall, these cumulative results indicate that BdP could support the production of cultured mussels at the baseline stocking level over the whole ADZ. The level of food depletion (< 10 %) predicted for the scenario based on twice the baseline stocking and 44 cm sock spacing is lower than the depletion predicted in Grande-Entrée Lagoon (Guyondet et al. 2010) and also than the depletion predicted in the present study at farm-scale for the

maximum capacity scenario (L =120 m and d = 3937 ind m^{-2}). As mentioned earlier, the individual mussel growth for this scenario was still within the limits of the observed growth variability. Hence, the depletion model results suggest that a 150 % increase in stock (equivalent to doubling the stocking density (doubling the sock length) and reducing the sock spacing from 55 to 44 cm) could be supported without any major change to the production cycle (i.e. no significant extension of the growing period).

These estimates do not account for any mussel feedback on their food production rate, although mechanisms such as increased nutrient turnover due to mussel excretion may increase the rate of phytoplankton turnover (Prins et al. 1998, Cranford et al. 2007). While a negligible influence is expected at the farm-scale where hydrodynamics and mussel filtration drive food availability, the development of a more complex ecosystem model would be necessary to estimate the magnitude of these feedback processes at the ADZ scale. However, a bulk calculation assuming a constant current of 8 cm s^{-1} perpendicular to the long axis of the ADZ leads to a water renewal time of less than 9 h for the whole ADZ volume. Hence, hydrodynamics are also likely of greater importance to mussel food turnover than is local production at the ADZ scale.

CONCLUSIONS

A numerical modelling approach based on in situ observations characterizing environmental conditions (water temperature, phytoplankton concentration and current velocity) was applied to compare the relevant time scales for the estimate of mussel production carrying capacity (water renewal time, organic seston turnover time and mussel clearance time) in a dynamic and integrative framework.

In BdP, the farm-scale evaluation led to the conclusion that the typical farm stock could be increased by a factor of 3 (although such a stocking would be impossible to achieve with present culture techniques) without causing much change to the production cycle and would increase production by a factor 2.5. Furthermore, the use of 120-m longlines, if enabled by a new anchorage system, would best match the BdP conditions and could increase mussel production by a further 12 %.

When this theoretical maximum stock scenario is scaled up from the farm to the whole ADZ, reduction in mean food availability is predicted to reach up to 30% over a very limited area and depletion conditions are constrained within the ADZ. Combining both the farm- and bay-scale evaluations, it was concluded that a scale-up of current stocking levels to the ADZ with an additional 150 % would still be within the limits of the production carrying capacity of BdP. Moreover it seems unlikely that this limit could be reached with present culture techniques.

Nonetheless, monitoring conditions in the ADZ, in particular mussel growth, which has been shown to be a good indicator of ecosystem status (Filgueira et al. 2014), while new farms are added, is strongly recommended to ensure the sustainable development of mussel aquaculture in BdP. In addition, climatic conditions appear to be changing rapidly in the area and, as pointed out by

Melaku Canu et al. (2010) and Callaway et al. (2012), this may considerably change the carrying capacity of areas for bivalve culture. Future work could consider this aspect under a variety of IPCC climate change scenarios to evaluate the longer-term sustainability of the practice in BdP.

ACKNOWLEDGEMENTS

This project was funded by DFO's Aquaculture Collaborative Research and Development Program (ACRDP project Q-13-01-001).

REFERENCES

Bourque, F., and Myrand, B. 2014. Potentiel de production mytilicole en milieu ouvert aux Îles-de-la-Madeleine. Merinov - Rapport de Recherche et Développement 14-09. 34 p.

Callaway, R., Shinn, A.P., Grenfell, S.E., Bron, J.E., Burnell, G., Cook, E.J., Crumlish, M., Culloty, S., Davidson, K., Ellis, R.P., Flynn, K.J., Fox, C., Green, D.M., Hays, G.C., Hughes, A.D., Johnston, E., Lowe, C.D., Lupatsch, I., Malham, S., Mendzil, A.F., Nickell, T., Pickerell, T., Rowley, A.F., Stanley, M.S., Tocher, D.R., Turnbull, J.F., Webb, G., Wootton, E., and Shields, R.J. 2012. Review of climate change impacts on marine aquaculture in the UK and Ireland. Aquat Conserv **22**: 389-421.

Cranford, P.J., Strain, P.M., Dowd, M., Hargrave, B.T., Grant, J., and Archambault, M.-C. 2007. Influence of mussel aquaculture on nitrogen dynamics in a nutrient enriched coastal embayment. Mar Ecol Prog Ser **347**: 61-78.

Dame, R.F., and Prins, T.C. 1997. Bivalve carrying capacity in coastal ecosystems. Aquat Ecol **31**: 409-421.

Department of Marine and Natural Resources. 2001. Guidelines for landscape and visual impact assessment of marine aquaculture, Dublin. p. 1-65.

Drapeau, G. 1988. Stability of tidal inlet navigation channels and adjacent dredge spoil islands. *In* Hydrodynamics and sediment dynamics of tidal inlets. *Edited by* D.G. Aubrey and L. Weishar. Springer-Verlag, New York, Vol. 29. pp. 226-244.

Ferreira, J.G., Sequeira, A., Hawkins, A.J.S., Newton, A., Nickell, T.D., Pastres, R., Forte, J., Bodoy, A., and Bricker, S.B. 2009. Analysis of coastal and offshore aquaculture: Application of the FARM model to multiple systems and shellfish species. Aquaculture **289**: 32-41.

Filgueira, R., Guyondet, T., Comeau, L.A., and Grant, J. 2014. Physiological

indices as indicators of ecosystem status in shellfish aquaculture sites. Ecol Indic **39**: 134-143.

Foreman, M.G. 1977. Manual for tidal heights analysis and previsions. Pacific Marine Science Report 77-10. 101 p.

Fréchette, M., and Lefaivre, D. 1990. Discriminating between food and space limitation in benthic suspension feeders using self - thinning relationships. Marine Ecology Progress Series **65**: 15-23.

Gauthier-Clerc, S., Tita, G., Bourque, F., Tremblay, R., Pellerin, J., Fournier, M., St-Louis, R., and Pelletier, E. 2007. Comparaison de la gamétogénèse de la moule bleue (*Mytilus edulis*) en mer et en lagune aux Îles-de-la-Madeleine. Rapport Scientifique - Université du Québec à Rimouski. 30 p.

Giles, H., Broekhuizen, N., Bryan, K.R., and Pilditch, C.A. 2009. Modelling the dispersal of biodeposits from mussel farms: The importance of simulating biodeposit erosion and decay. Aquaculture **291**: 168-178.

Godin, G. 1979. La marée dans le Golfe et l'Estuaire du Saint-Laurent. Le Naturaliste Canadien **106**: 105-121.

Goulletquer, P., and Le Moine, O. 2003. Shellfish farming and Coastal Zone Management (CZM) development in the Marennes-Oléron Bay and Charentais Sounds (Charente Maritime, France): A review of recent developments. Aquacult Int **10**: 507-525.

Guyondet, T., and Koutitonsky, V.G. 2008. Tidal and residual circulations in coupled restricted and leaky lagoons. Estuar Coast Shelf S **77**: 396-408.

Guyondet, T., Roy, S., Koutitonsky, V.G., Grant, J., and Tita, G. 2010. Integrating multiple spatial scales in the carrying capacity assessment of a coastal ecosystem for bivalve aquaculture. J Sea Res **64**: 341-359.

Guyondet, T., Sonier, R., and Comeau, L.A. 2013. Spatially explicit seston depletion index to optimize shellfish culture. Aquacult Environ Interact **4**: 175-186.

Heip, C.H.R., Goosen, N.K., Herman, P.M.J., Kromkamp, J., Middelburg, J.J., and Soetaert, K. 1995. Production and consumption of biological particles in temperate tidal estuaries. Oceanogr Mar Biol **33**: 1-149.

Inglis, G.J., Hayden, B.J., and Ross, A.H. 2000. An overview of factors affecting the carrying capacity of coastal embayments for mussel culture CHC00/69. NIWA, Christchurch, New Zealand. 38 p.

King, I.P. 1982. A finite element model for three dimensional flow. report prepared by Resource Management Associates, Lafayette California, for U.S. Army Corps of Engineers, Waterways Experiment Station, Vicksburg, Mississippi.

Kooijman, S.A.L.M. 2000. Dynamic energy and mass budgets in biological systems. Cambridge University Press, Cambridge. 424 p.

Koutitonsky, V.G., Guyondet, T., St-Hillaire, A., Courtenay, S.C., and Bohgen, A.D. 2004. Water renewal estimates for aquaculture developments in the Richibucto Estuary, Canada. Estuaries **27**(5): 839-850.

Koutitonsky, V.G., Navarro, N., and Booth, D. 2002. Descriptive Physical Oceanography of Great-Entry Lagoon, Gulf of St. Lawrence. Estuar Coast Shelf S **54**: 833-847.

Longdill, P.C., Healy, T.R., and Black, K.P. 2008. An integrated GIS approach for sustainable aquaculture management area site selection. Ocean Coast Manage **51**: 612-624.

McKindsey, C.W., Thetmeyer, H., Landry, T., and Silvert, W. 2006. Review of recent carrying capacity models for bivalve culture and recommendations for research and management. Aquaculture **261**: 451-462.

Melaku Canu, D., Solidoro, C., Cossarini, G., and Giorgi, F. 2010. Effect of global change on bivalve rearing activity and the need for adaptive management. Mar Ecol Prog Ser **42**: 13-26.

Petersen, J.K., Nielsen, T.G., van Duren, L., and Maar, M. 2008. Depletion of plankton in a raft culture of *Mytilus galloprovincialis* in Ria de Vigo, NW Spain. I. Phytoplankton. Aquat Biol **4**: 113-125.

Prins, T.C., Smaal, A.C., and Dame, R.F. 1998. A review of feedbacks between bivalve grazing and ecosystem processes. Aquat Ecol **31**: 349-359.

Rosland, R., Bacher, C., Strand, Ø., Aure, J., and Strohmeier, T. 2011. Modelling growth variability in longline mussel farms as a function of stocking density and farm design. J Sea Res **66**: 318-330.

Rosland, R., Strand, Ø., Alunno-Bruscia, M., Bacher, C., and Strohmeier, T. 2009. Applying Dynamic Energy Budget (DEB) theory to simulate growth and bio-energetics of blue mussels under low seston conditions. J Sea Res **62**: 49-61.

Stead, S.M., Burnell, G., and Goulletquer, P. 2002. Aquaculture and its role in Integrated Coastal Zone Management. Aquacult Int **10**: 447-468.

Stevens, C., Plew, D., Hartstein, N., and Fredriksson, D. 2008. The physics of open-water shellfish aquaculture. Aquacult Eng **38**(3): 145-160.

Strickland, J.D.H., and Parsons, T.R. 1972. A practical handbook of seawater analysis. Bulletin 167: Fisheries research board of Canada.

Strohmeier, T., Aure, J., Duinker, A., Castberg, T., Svardal, A., and Strand, Ø. 2005. Flow reduction, seston depletion, meat content and distribution of diarrhetic shellfish toxins in a long-line blue mussel (*Mytilus edulis*) farm. J Shellfish Res **24**: 15-23.

Trottet, A., Roy, S., Tamigneaux, E., and Lovejoy, C. 2007. Importance of heterotrophic planktonic communities in a mussel culture environment: the Grande-Entrée Lagoon, Magdalen Islands (Québec, Canada). Mar Biol **151**: 377-392.

van der Veer, H.W., Cardoso, J.F.M.F., and van der Meer, J. 2006. The estimation of DEB parameters for various Northeast Atlantic bivalve species. J Sea Res **56**: 107-124.

Weise, A.M., Cromey, C.J., Callier, M.D., Archambault, P., Chamberlain, J., and McKindsey, C.W. 2009. Shellfish-DEPOMOD: Modelling the biodeposition from suspended shellfish aquaculture and assessing benthic effects. Aquaculture **288**: 239-253.

Werstink, G. 2007. Évaluation du potentiel conchylicole des Îles-de-la-Madeleine (Québec, Canada): une analyse multicritères combine à un système informatique géographique. MSc Thesis, Université du Québec à Rimouski.

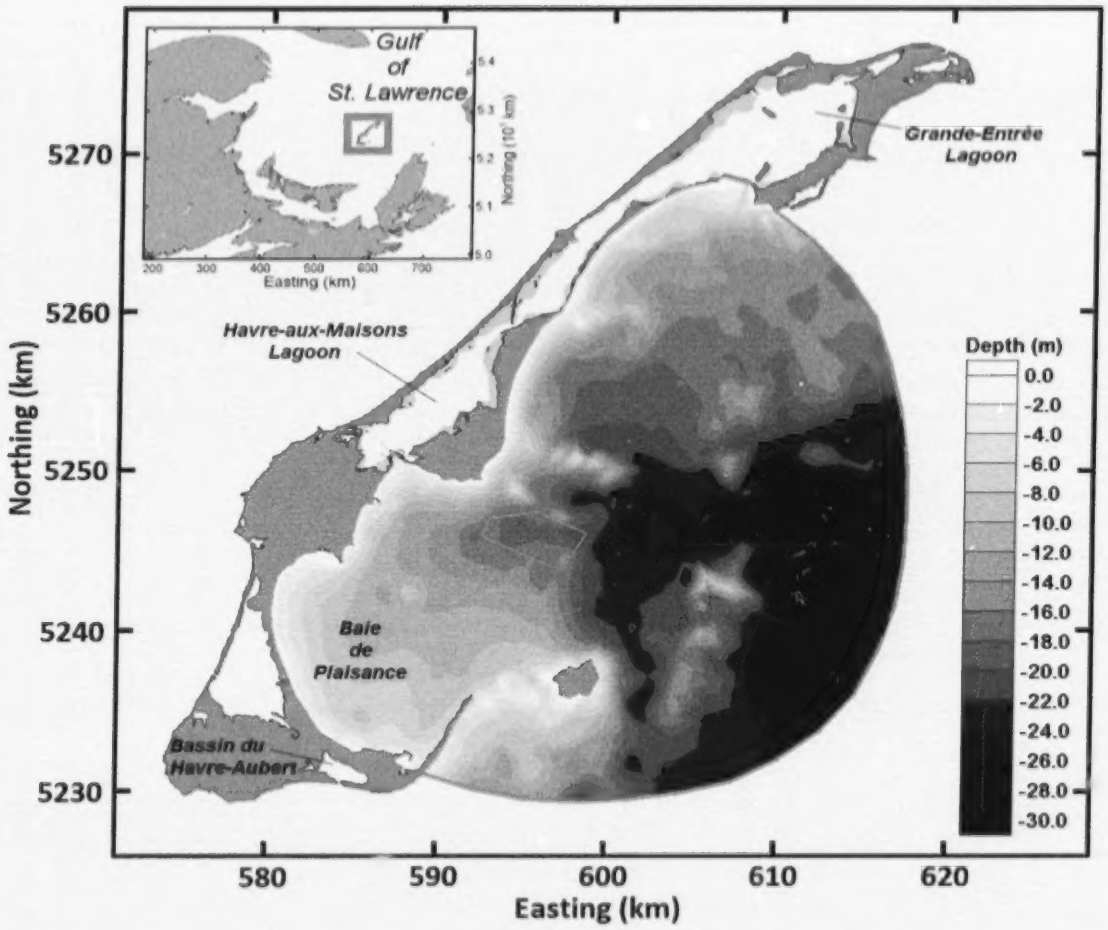

Figure 1. Map of the study area showing the bathymetry within the Baie de Plaisance (BdP) hydrodynamic model domain and the location of the aquaculture development zone (ADZ; red polygon).

Typical Farm Layout

with: - 50m transversal spacing
- 90m longitudinal spacing due to mooring length (2 x 45m)
- 3m mussel socks

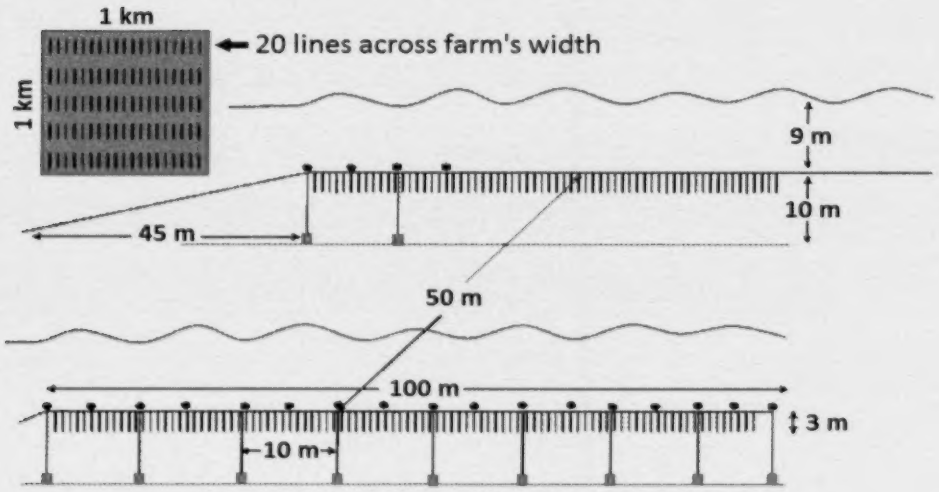

Figure 2. Sketch of typical farm layout currently used by the commercial mussel farm in BdP.

Figure 3. Location of the 2001 tide gauges (L1, 9, 10, 11, 12) from Guyondet and Koutitonsky (2008) and 2013 current meters, CTD and water sampling stations (ADCP1 and 2). The contours of the ADZ (dashed line) and of the farm currently in operation (bold line) are also reported.

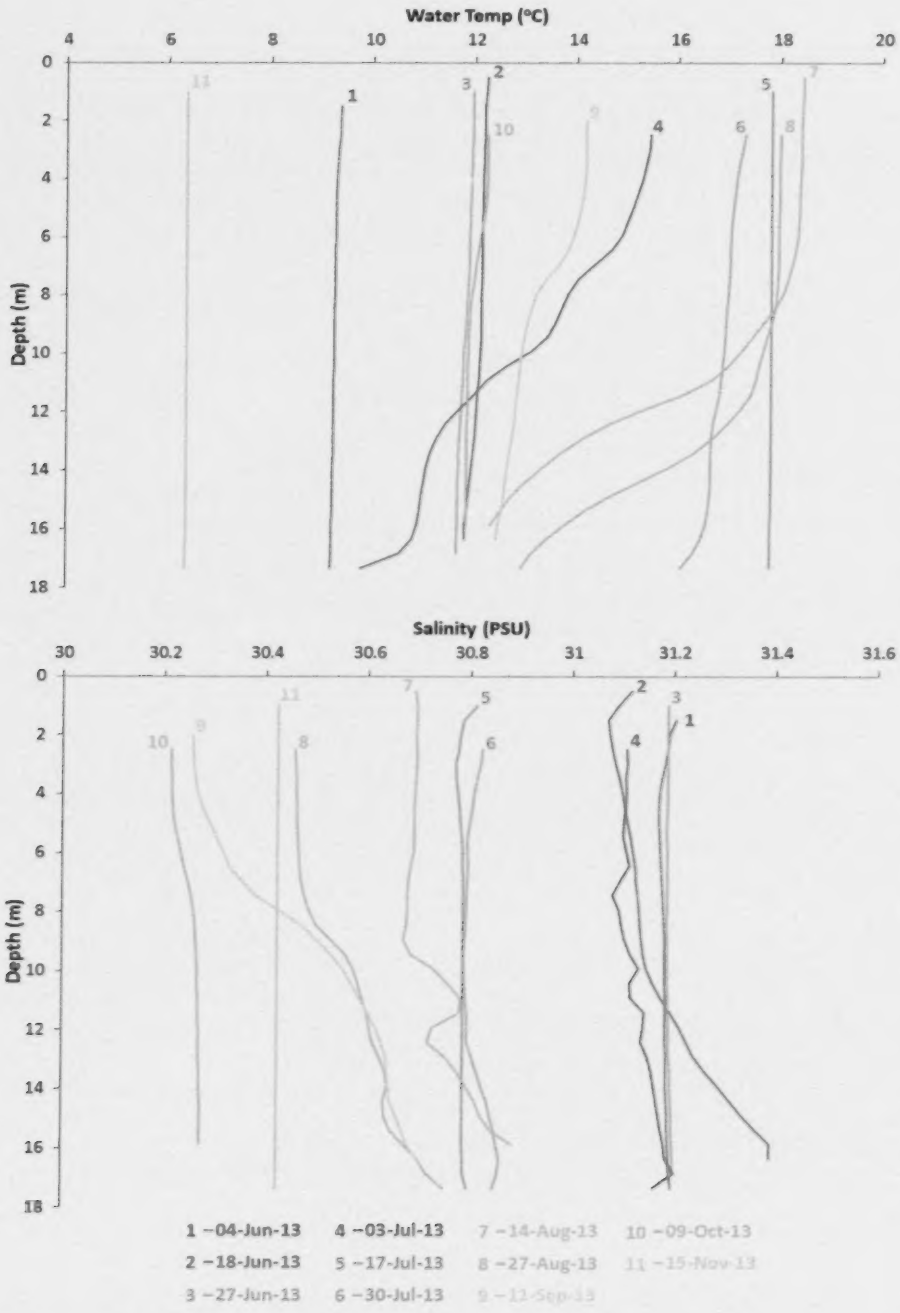

Figure 4. Vertical profiles of water temperature (top panel) and salinity (bottom panel) at station ADCP2 during the whole 2013 sampling period.

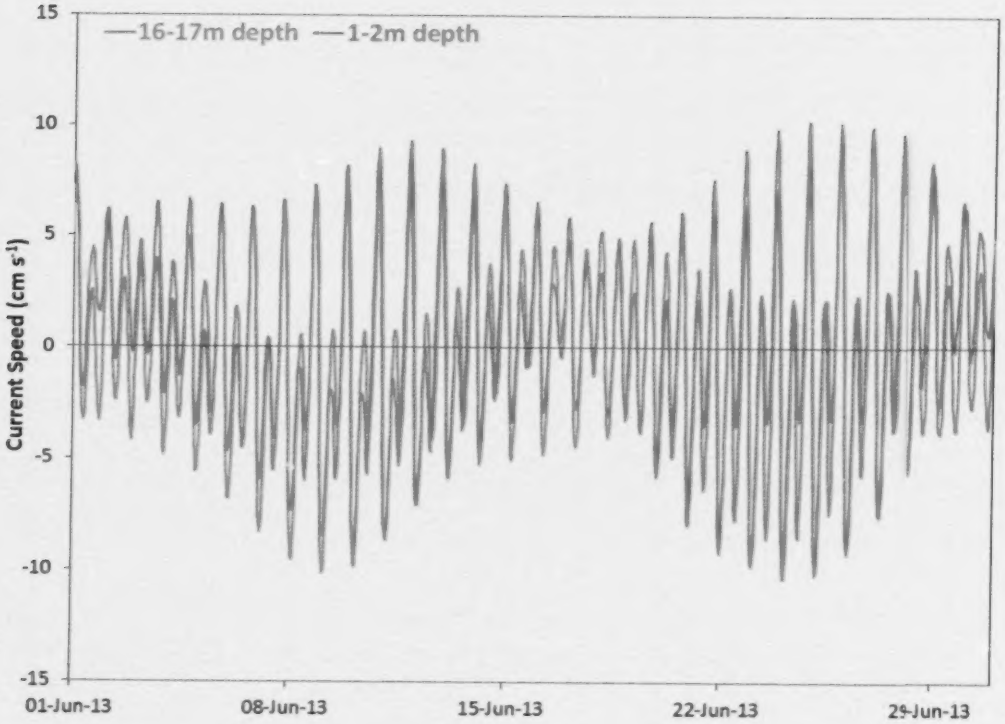

Figure 5. Comparison of tidal current time series at the top and bottom of the water column at station ADCP2 during the month of June 2013.

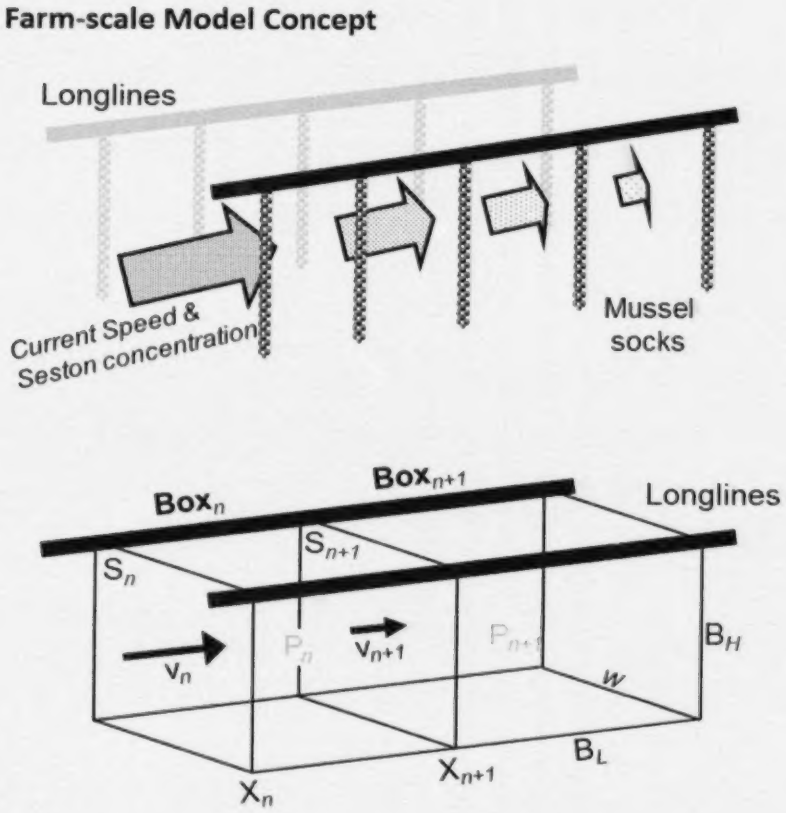

Figure 6. Sketch of farm-scale model configuration with x axis oriented along the longlines and box dimensions (length B_L = 1/10 of longline length (L), width or line spacing w and mussel sock length B_H) for which current velocity (v) and seston concentration (P) are calculated.

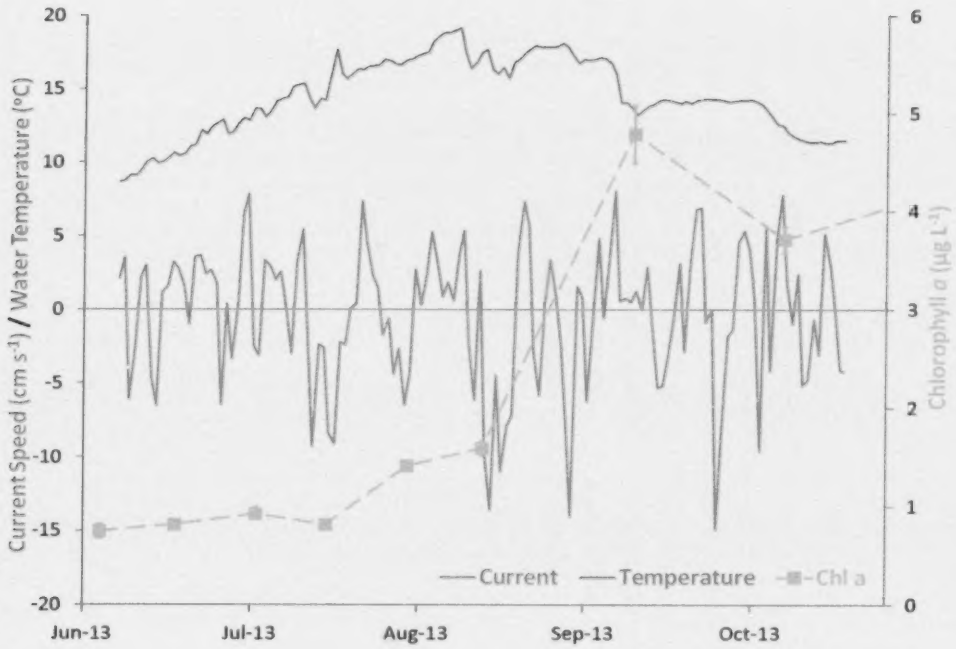

Figure 7. Time series of environmental conditions (water temperature, phytoplankton concentration (Chl *a*) and current velocity) used to force the farm-scale model and obtained from the analysis of CTD, ADCP current meter, and water sample data collected at station ADCP2 during summer-fall 2013.

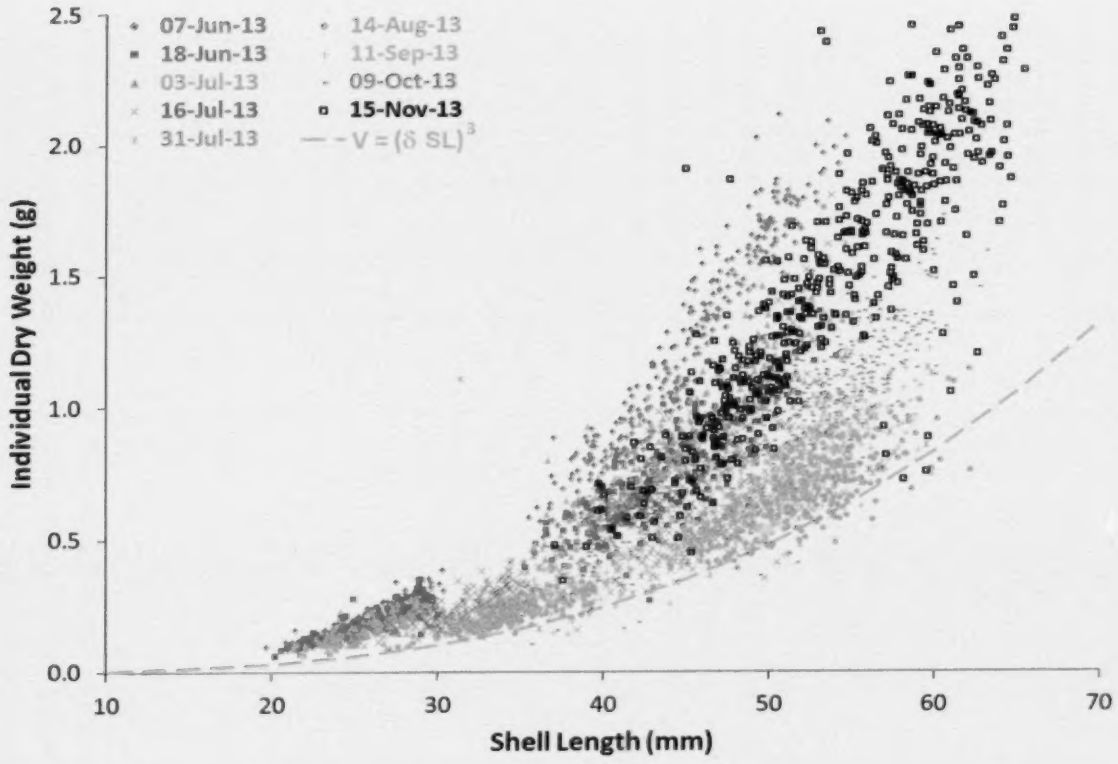

Figure 8. Shell length – Individual dry weight relation for all individual mussels collected during the course of the 2013 field study for growth measurements. The relationship Volume (V) – Shell length (SL) used in the Dynamic Energy Budget (DEB) is also reported for the calibrated value of the shape parameter (δ).

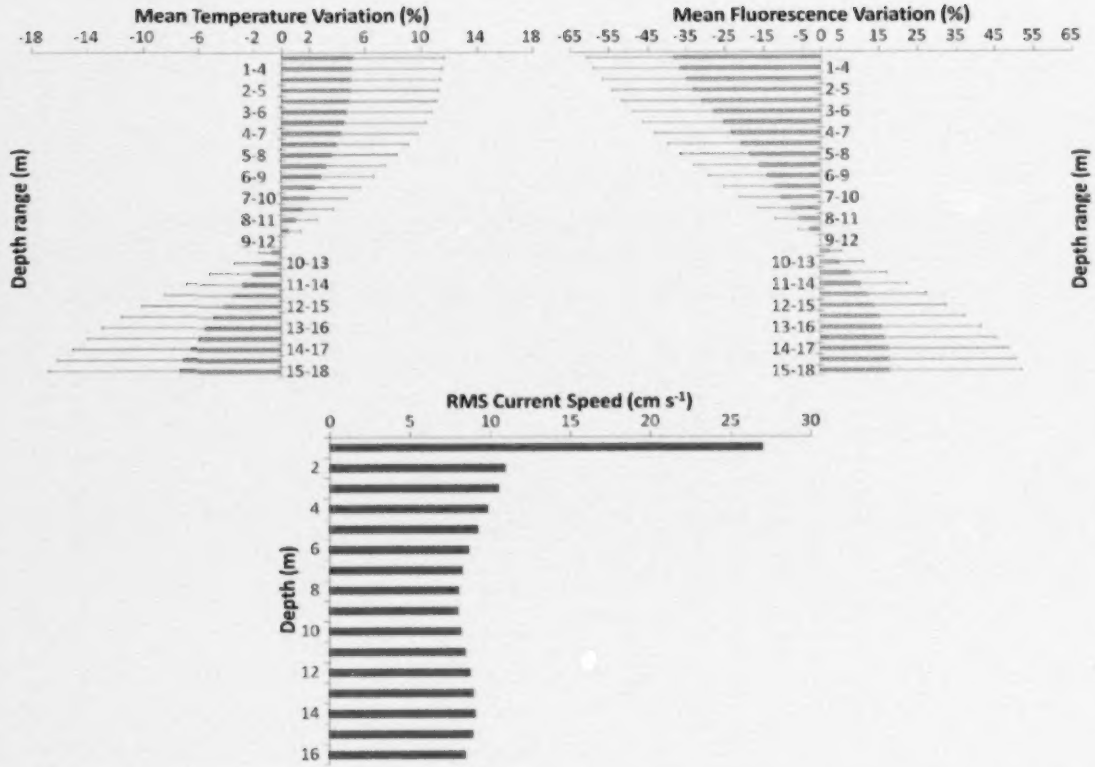

Figure 9. Mean vertical structure of the water column during the study period at station ADCP2 in terms of water temperature (top left panel) and phytoplankton concentration (measured as fluorescence, top right panel). These observations are reported for 3-m depth ranges with 0.5 m increments and expressed as relative variation compared to the 9-12 m layer. The bottom panel gives the vertical structure in mean (Root Mean Square, RMS) current velocity at 1 m intervals.

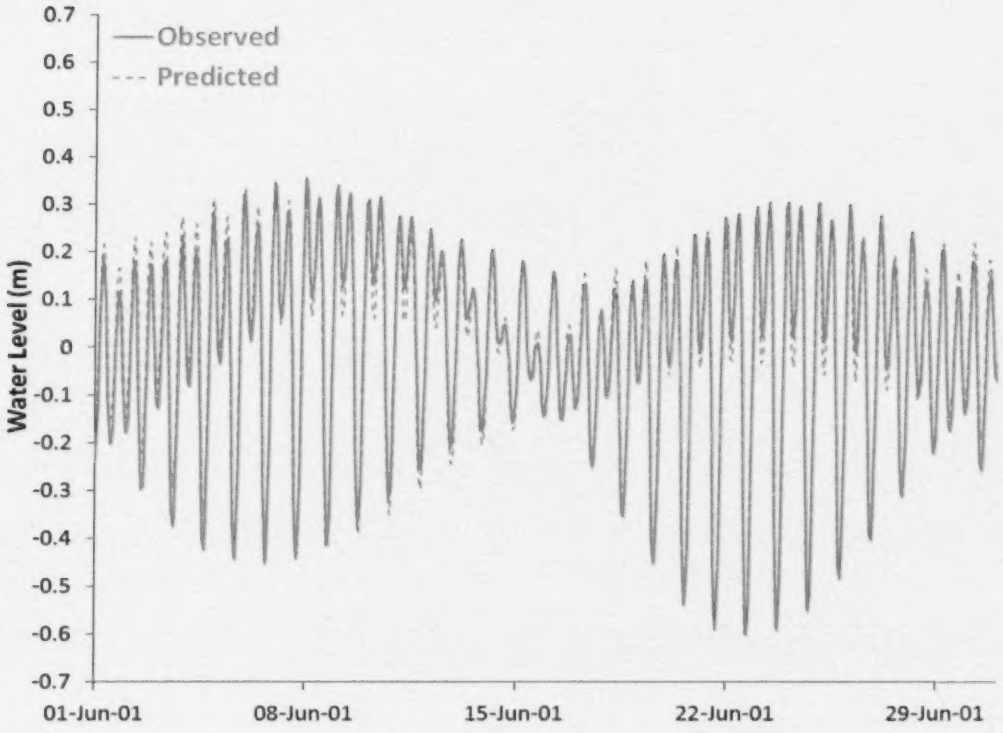

Figure 10. Hydrodynamic model validation. Comparison of observed and predicted tidal water level fluctuation time series at station L12 during the month of June 2001.

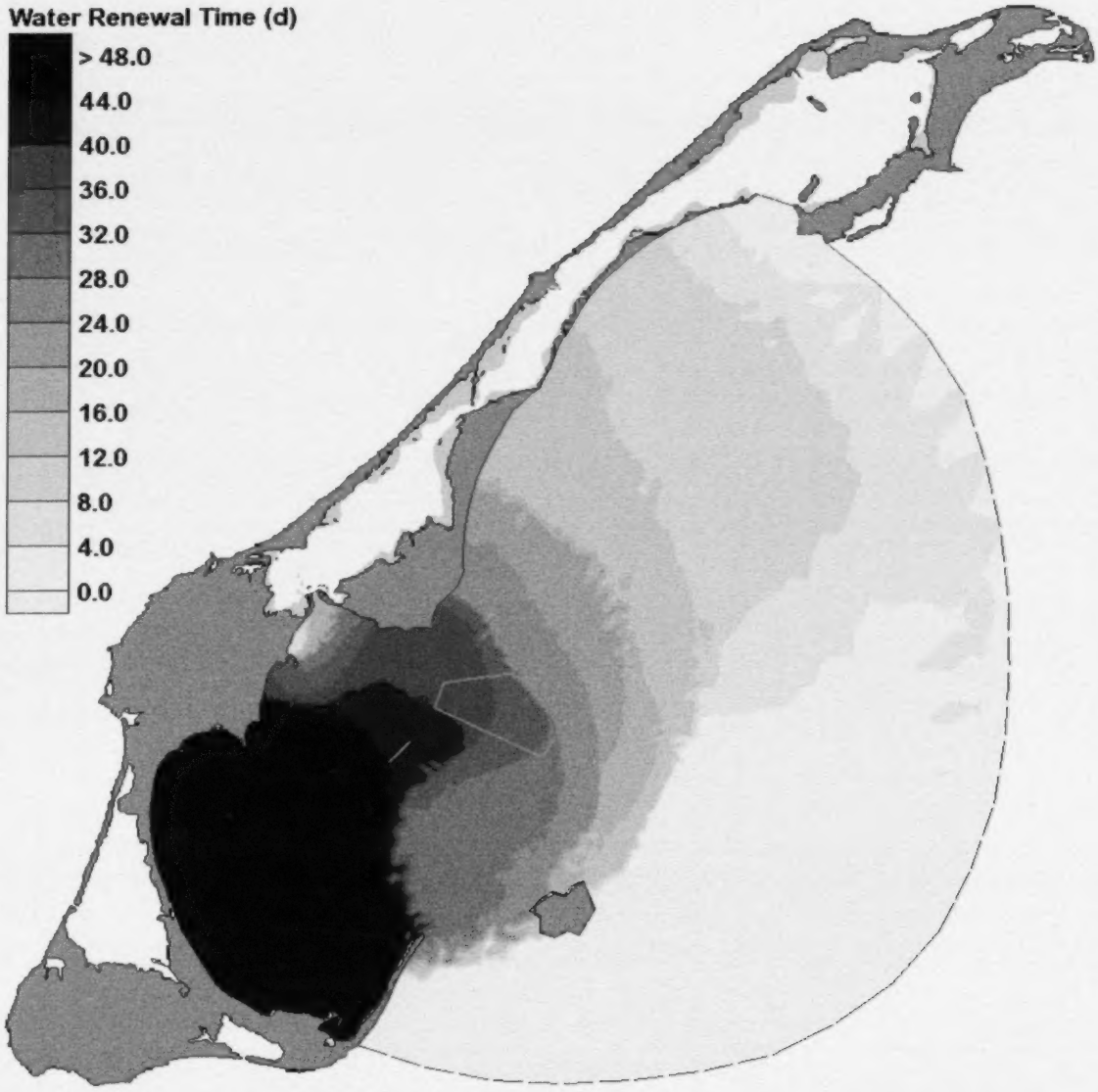

Figure 11. Spatial distribution of water renewal time over BdP from the hydrodynamic model results and the tracer advection-dispersion method.

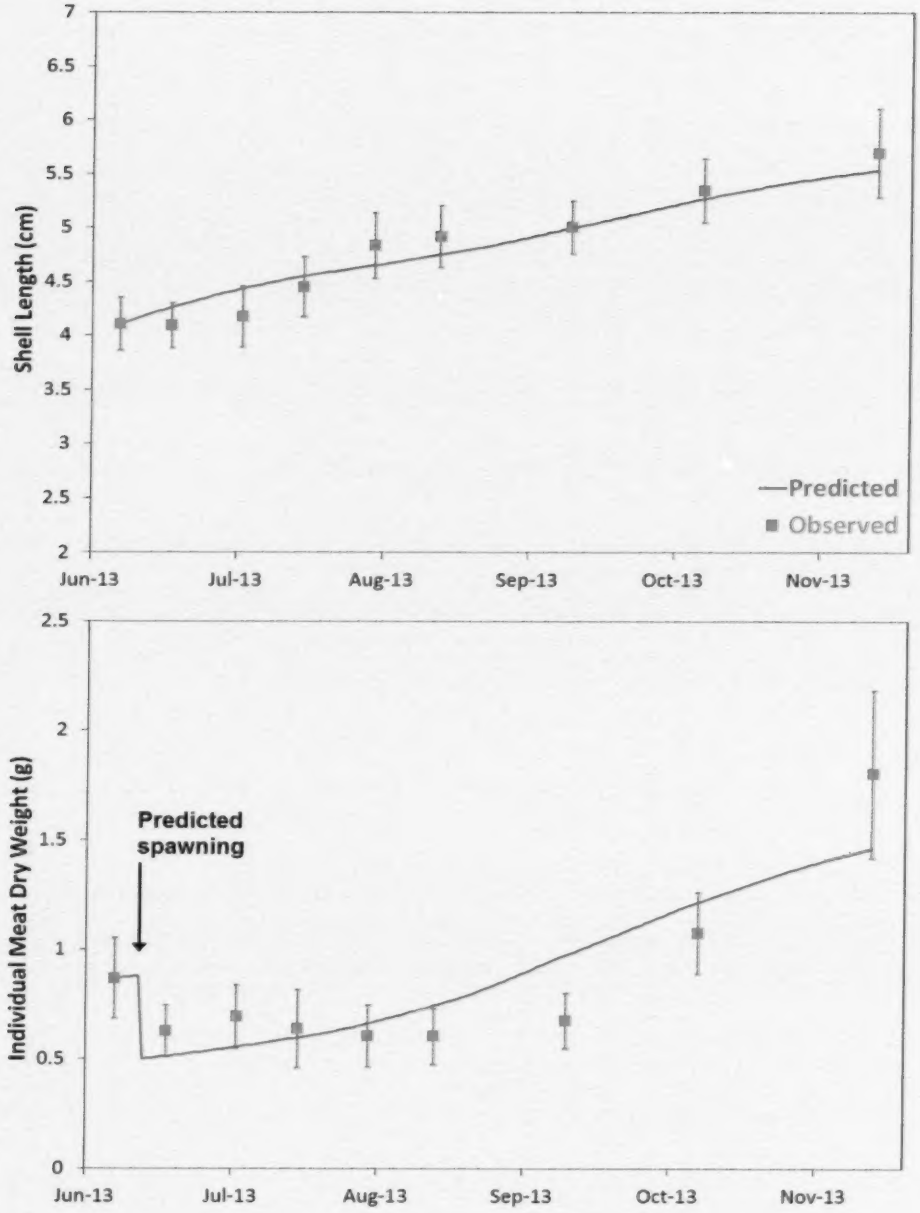

Figure 12. DEB model validation. Comparison of observed and predicted mussel growth both in terms of shell length (top panel) and dry meat weight (bottom panel). Mean observed values are reported along with ± 1 standard deviation.

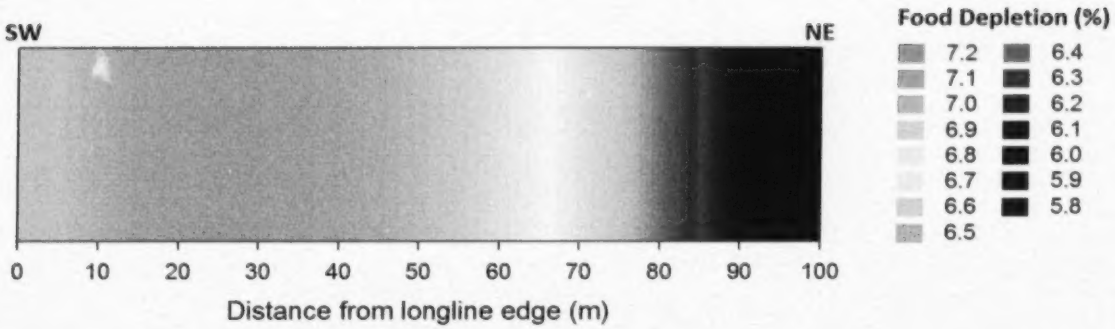

Figure 13. Distribution of food depletion along a typical longline corridor as reproduced by the farm-scale model in response to the combine effects of food replenishment by water circulation and food consumption by mussel filtration. Food depletion is calculated as the relative difference between food concentration inside the farm and the outside forcing concentration.

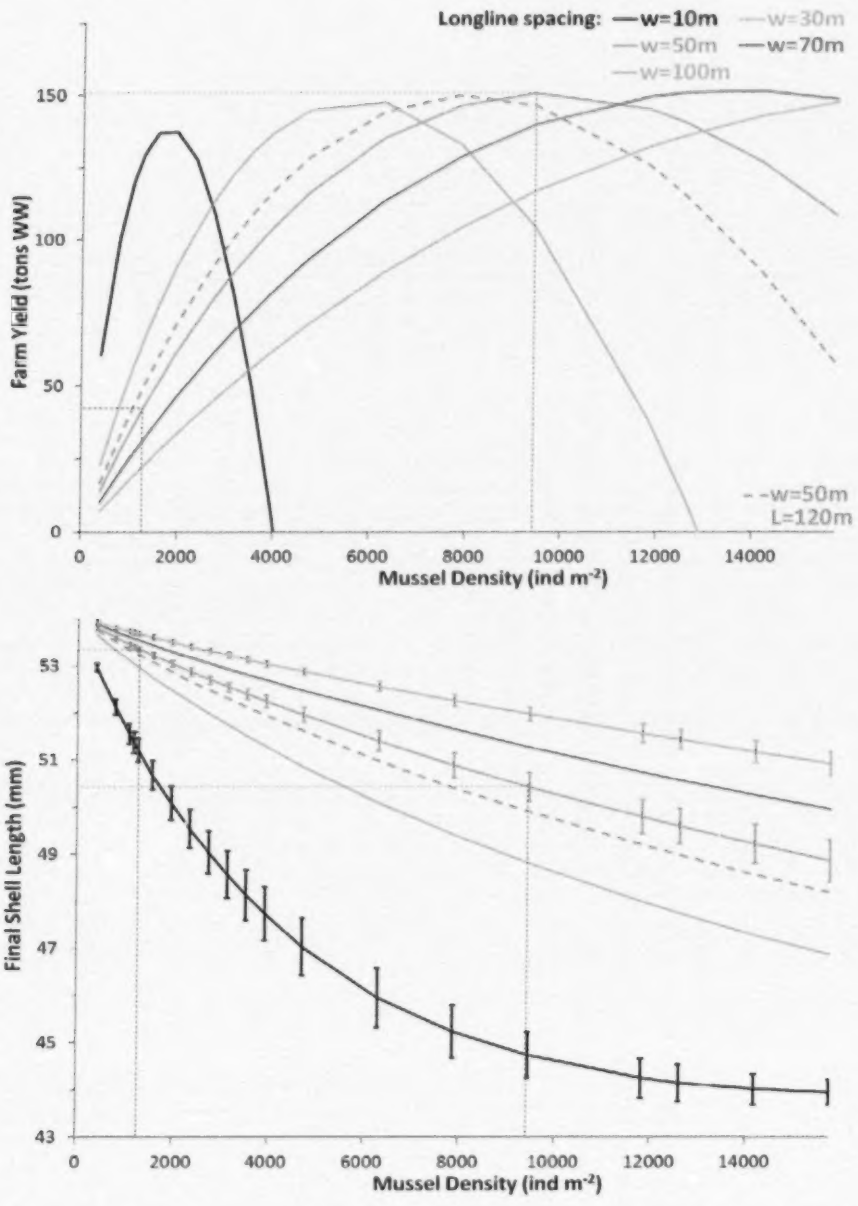

Figure 14. Farm-scale model results. Effects of stocking density and longline spacing (w) on total farm yield (top panel) and individual mussel growth (bottom panel) reported as the shell length at the end of the simulation period (error bars represent spatial variability within the farm and for clarity are only included for the minimum, maximum and current line spacing scenarios). Farm yield and final shell length obtained at w = 50 m are indicated (dotted lines) for both current and maximum production scenarios. The planned configuration (L = 120 m and w = 50 m) is also presented (dashed red line).

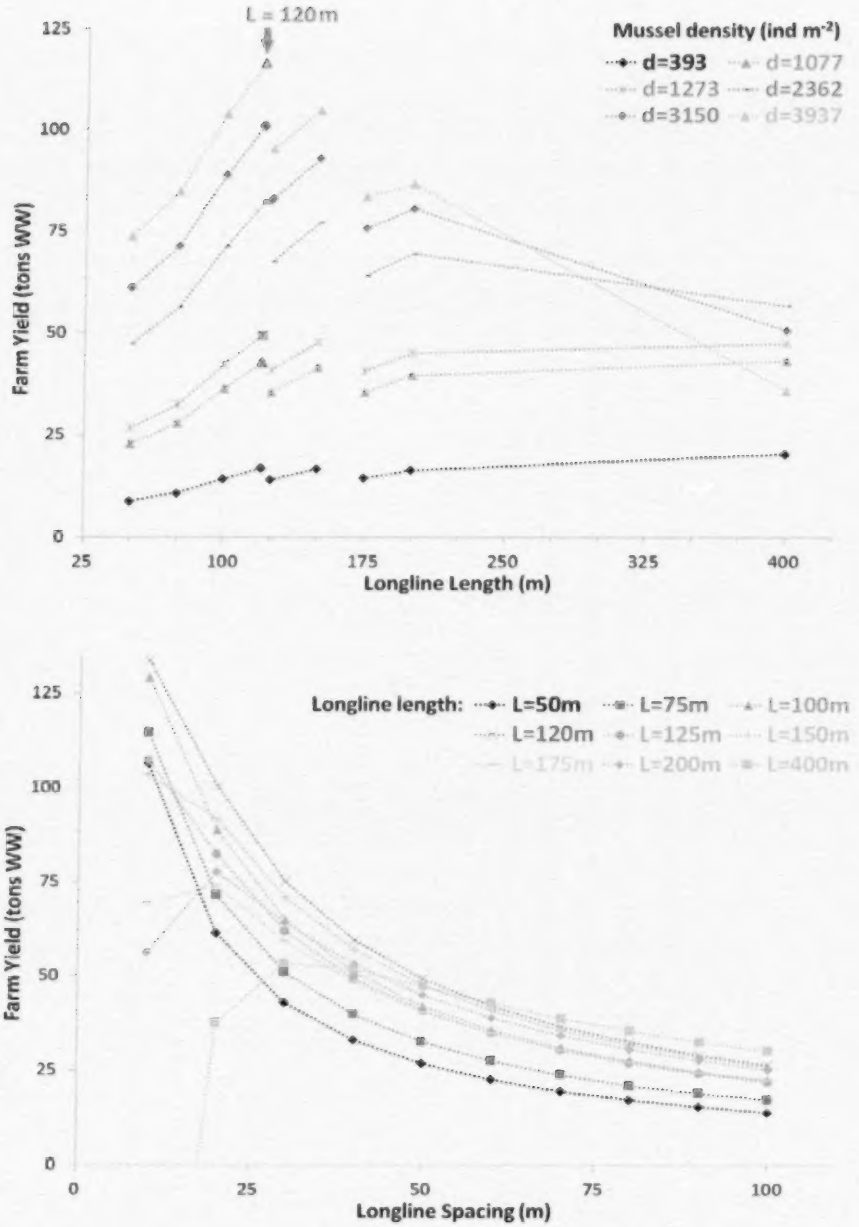

Figure 15. Farm-scale model results. Effects of longline length (L) and stocking density on total farm yield (top panel; see text for broken line meaning) showing the optimum reached for L = 120 m (longline length planned with technological development). Effects of longline length and spacing on total farm yield (bottom panel) also showing optimum for L = 120 m and spacing w < 60m.

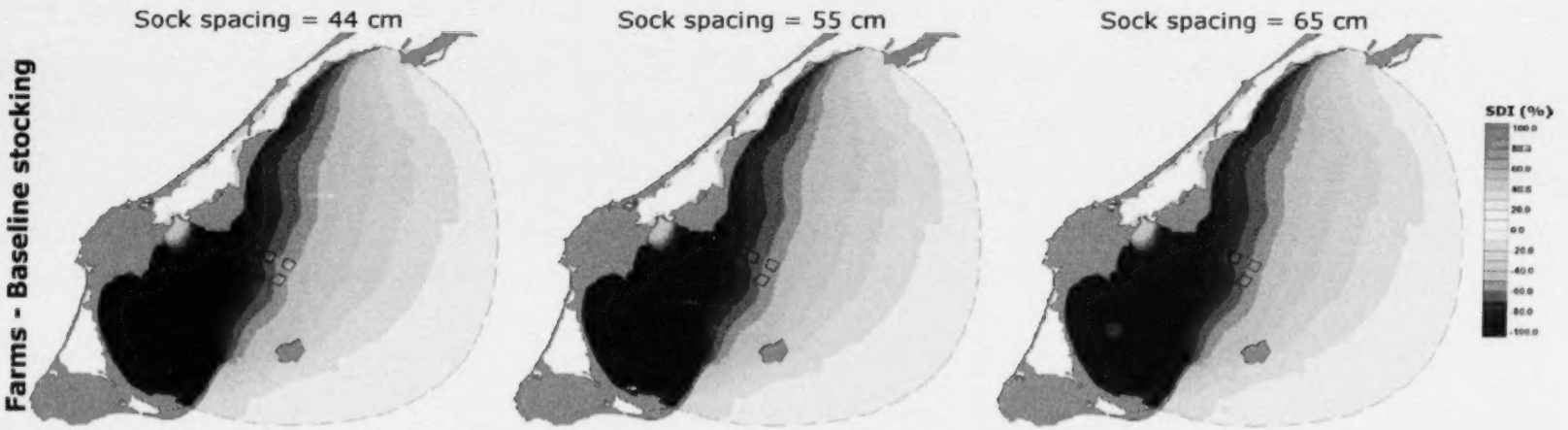

Figure 16. Depletion model results. Effects of 4 isolated typical farms on the spatial distribution of food depletion in three sock spacing scenarios (44, 55 and 65 cm). Food depletion is expressed as the seston depletion index SDI. SDI > 0 denotes an actual depletion while SDI <0 follows an accumulation of seston compared to the boundary constant value. Black polygons delineate the farms.

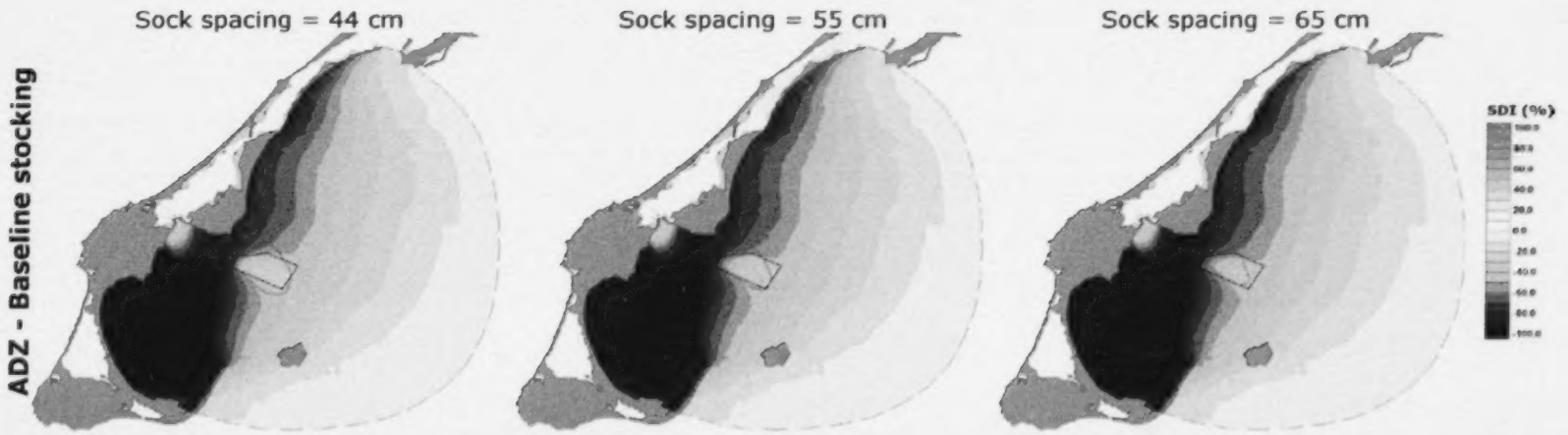

Figure 17. Depletion model results. Spatial distribution of SDI over BdP for the case where the typical farm design is extended over the whole ADZ and for the three sock spacing scenarios. Red contours delineate the maximum extent of depletion (SDI > 0) predicted over the course of the simulation period.

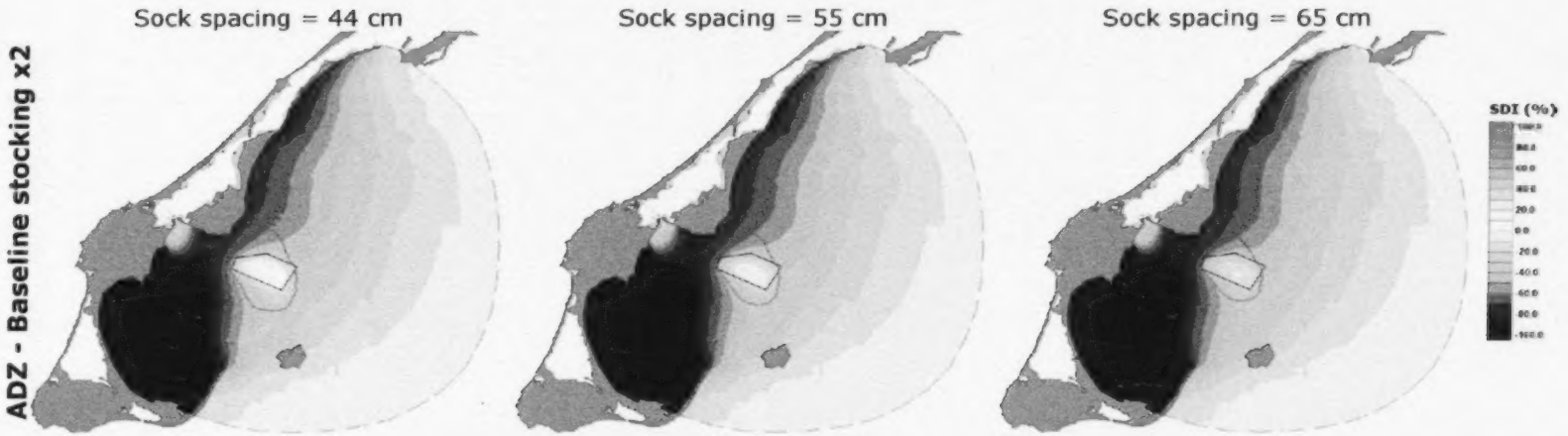

Figure 18. Depletion model results. Spatial distribution of SDI over BdP for the case where the typical farm design is extended over the whole ADZ with twice the baseline stocking density and for the three sock spacing scenarios. Red contours delineate the maximum extent of depletion (SDI > 0) predicted over the course of the simulation period.

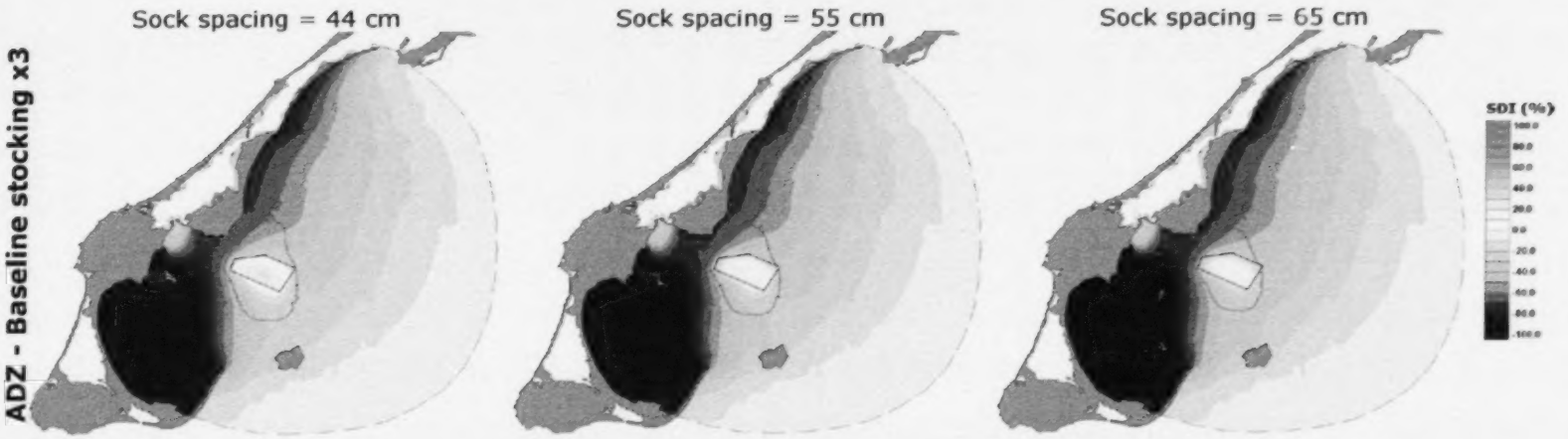

Figure 19. Depletion model results. Spatial distribution of SDI over BdP for the case where the typical farm design is extended over the whole ADZ with three times the baseline stocking density and for the three sock spacing scenarios. Red contours delineate the maximum extent of depletion (SDI > 0) predicted over the course of the simulation period.